

Density Functional Theory (DFT) Study on α,α -Bis(2-benzothiophen-1-yl)-4H-cyclopenta[2,1-b,3;4-b']dithiophene Derivatives for Optoelectronic Devices

Banjo Semire* and Olusegun Ayobami Odunola

Department of Pure and Applied Chemistry, Ladoké Akintola University of Technology, Ogbomosó, Oyo State, Nigeria

*Corresponding email: bsemire@lautech.edu.ng

Received 22 November 2018; Accepted 12 June 2019

ABSTRACT

Bis(2-benzothiophen-1-yl)-4H-cyclopenta[2,1-b,3;4-b']dithiophene derivatives comprised of three series; bis(2-thienyl)-4H-cyclopenta[2,1-b,3;4-b]dithiophene (BTDT), diphenyl-4H-cyclopenta[2,1-b,3;4-b]dithiophene (DPDT) and bis(2-benzothiophen-1-yl)-4H-cyclopenta[2,1-b,3;4-b]dithiophene (BBDT) have been studied using Density Functional Theory (B3LYP/6-31G**). In each series, molecules with C=S bridge exhibited the lowest band gap; for instance in BBDT series, the energy band gap could be arranged as 2.29, 2.23 and 1.66 eV for CH₂, C=O and C=S bridge respectively. The low band gaps calculated for BBDT-C=S (1.66 eV) and BTDT-C=S (1.82 eV) could facilitate photo-excited electron transfer as one the criteria for a molecule to be used in photovoltaic devices. Also, the results showed that longest UV-vis absorption wavelength was observed for molecules with C=S bridge, i.e. 1013.66, 874.75 and 1097.66 nm for BTDT, DPDT and BBDT respectively. The polarizability (α_0) values calculated for the molecules follow as -CH₂ < C=O < C=S bridge in each series, indicating that the higher the polarizability (α_0) value the longer the λ_{max} nm and the lower the energy band gap. The magnitude of the molecular hyperpolarizability β_0 showed that molecular structures with -C=O bridge could be best NLO material in each series.

Keywords: α,α -bis(2-benzothiophen-1-yl)-4H-cyclopenta[2,1-b,3;4-b']dithiophene; electronic properties, NLO, DFT

INTRODUCTION

Since the discovery of organic π -conjugated molecules, polythiophenes have become one of the most interesting research topics in the fields of chemistry physics and materials science as most promising materials for the optoelectronic device technology, such as LEDs, p-channel transistors (TFTs), and solar cell [1-10]. The eligibility of oligothiophenes (π -center) for potential property modulator is associated with the role of sulfur d-orbitals that mix well with aromatic p-orbitals [11,12]. However, polythiophenes are highly amorphous; oligothiophenes are not amorphous and can be synthesized as well defined compounds. Recently, many researchers have become interested in synthesizing short-chain optoelectronic compounds based on oligothiophenes [13-18]. This has led to modeling of low molecular weight thiophene based molecules using various theoretical methods to design thiophene derivatives with superior quality as optoelectronic molecules [17, 19-21]. One of such research was the study

The journal homepage www.jpacr.ub.ac.id
p-ISSN : 2302 – 4690 | e-ISSN : 2541 – 0733

of some bridged oligothiophene octamers with bridges containing electron-accepting groups [22-25] and bridged dithiophene S-oxide analogues [26-28].

Therefore, in this work, the structure and electronic properties of bis(2-benzothiophen-1-yl)-4H-cyclopenta[2,1-b,3;4-b]dithiophene (BBDT), diphenyl-4H-cyclopenta[2,1-b,3;4-b]dithiophene (DPDT) and bis(2-thienyl)-4H-cyclopenta[2,1-b,3;4-b]dithiophene (BTDT) derivatives with CH₂, C=S, C=O bridge are examined. These light weight molecules are modeled in order to modulate the band gap which is one of the intrinsic properties of conducting materials.



Figure 1. Schematic structure and atomic numbering of studied molecules: X = CH₂, C=S, C=O and A = thiophene, 2-benzothiophene or benzene

EXPERIMENT

Computational methods

The equilibrium geometries and the frequencies for all the studied molecules were fully optimized at density functional theory (Beckes's three-parameter hybrid functional [29]) employing the Lee, Yang and Parr correlation functional B3LYP [30]). The basis set 6-31G** was used for all atoms in the calculations. Single point energy calculations were performed on the optimized geometries of these molecules at DFT level of theories. The absorption transitions were calculated from the optimized geometry in the ground state S₀ using TD-B3LYP/6-31G**. The convergence criteria for the energy calculations and geometry optimizations used in the density functional methods were default parameters in the Spartan 14 program [31].

RESULT AND DISCUSSION

Geometries

The schematic structure of the studied molecules with numbering displayed in Figure 1 are in three series namely BBDT-X, DPDT-X and BTDT-X (where X is the bridge). The geometries of these molecules calculated at B3LYP/6-31G** are shown in Table 1. The effect of X and A on the π -center geometry (i.e. 4H-cyclopenta[2,1-b,3;4-b]dithiophene) would be discussed separately for proper understanding. In the Table 1, both X and A have effect on the π -center geometry, although X has profound much effect. For a particular X, say CH₂, the geometries of BBDT and BTDT are similar but quite different from that of DPDT. The major differences observed in bond lengths for both BBDT and BTDT are S-C, C₄-C₅ and C-A bonds. For instance, C₁-S₁ (C₅-S₂), C₄-C₅ and C₁-A are 1.776Å (1.727Å), 1.438Å and 1.446Å for BBDT and 1.772Å (1.725Å), 1.435Å and 1.445Å for BTDT. However, in terms of bond angles and dihedral angles, there are no significant differences in their bond angles of these molecules, though BBDT differs in dihedral angles compared to others. In general, the π -center of BBDT-CH₂, BTDT-C=O and DPDT-C=O are more planar than other molecules (Table 1).

Electronic properties

The highest occupied molecular orbital (HOMO), lowest unoccupied molecular orbital (LUMO) and HOMO-LUMO band gaps are shown in Figure 2. The band gaps for BBDT series are 2.29eV, 1.66eV and 2.23eV for BBDT-CH₂, BBDT-C=S and BBDT-C=O respectively.

For DPDT series, the band gaps are 3.33eV, 2.08eV and 2.69eV for DPDT-CH₂, DPDT-C=S and DPDT-C=O respectively. In case of BTDT series, the band gaps are 2.95eV, 1.82eV and 2.46eV for BTDT-CH₂, BTDT-C=S and BTDT-C=O respectively. Furthermore, there is destabilization of the HOMO and LUMO in the molecules with C=O and C=S bridges which led to lowering of band gaps compared to CH₂ bridge. This could be linked to the electron-withdrawing effect of C=S and C=O bridges. In each series, molecule with C=S bridge has lowest band gap. Therefore, the band gaps could be arranged in order C=S < C=O < CH₂. The BBDT molecules have the overall lowest band gaps (Figure 2). The calculated band gaps values for BBDT-C=S and BTDT-C=S lie within compounds employed in solar cells, i.e. band gap < 1.9 eV [32] and optical compounds [33,34]. Also, the LUMO energy levels of the these molecules are sufficiently higher than the conduction band edge of TiO₂ (-4.0 eV, [35]) and PCBM (-3.7 eV [36,37]), this could facilitate photo-excited electron transfer from these molecules to TiO₂ (or to PCBM) as one the criteria for a molecule to be used in photovoltaic devices. Figure 3 shows the frontier orbitals of the studied molecules, It is observed that the HOMOs are C=C bonding and C-C anti-bonding while the LUMOs are C-C bonding and C=C anti-bonding. The HOMO spreads over the entire molecule, however LUMO are essentially on π -center with contribution from lone pair electrons for C=O and C=S bridge.

The absorption peaks, oscillation strength and percentage of the molecular orbitals involved in transition calculated for BTDT, BBDT and DPDT at TD-B3LYP/6-31G** are displayed in Table 2. The oscillator strength values (O.S), a parameter that shows the probability of the transition (i.e. corresponding to a fraction of negative charges, electrons) which accomplishes the transition in question (oscillate) reveals that CH₂ bridge molecules have the highest probability of electrons transition from ground state to the excited state. Therefore, oscillator strength (OS) values < 0.005 are considered to be transition arising from low absorption bands in this paper. For BTDT series, BTDT-CH₂ has two strong absorption (i.e. > 0.005 O.S) at 270.85 and 413.51 nm arising from HOMO-2 \rightarrow LUMO (91%) and HOMO \rightarrow LUMO (97%) respectively; the longest λ_{\max} with highest O.S is characterized as π - π^* transition arising from HOMO \rightarrow LUMO. For BTDT-C=S, three strong absorption peaks are identified at 370.21, 392.42 and 1013.66 nm with O.S values of 0.7145, 0.6385 and 0.0478 respectively. The absorption peak with highest O.S is characterized as π - π^* and n- π^* transitions arise from HOMO-4 \rightarrow LUMO (73%) and HOMO \rightarrow LUMO+1 (21%); 392.42 nm peak arises from HOMO \rightarrow LUMO+1 (64%), HOMO-4 \rightarrow LUMO (20%) and HOMO-6 \rightarrow LUMO (11%) and 1013.66 nm peak arises from HOMO \rightarrow LUMO (97%). For BTDT-C=O, 317.60, 363.64 and 613.57 nm are three absorption peaks with O.S higher than 0.005 arising from HOMO-2 \rightarrow LUMO (70%) and HOMO-4 \rightarrow LUMO+1 (16%) for 317.60 nm absorption peak, HOMO \rightarrow LUMO+1 (89%) for 363.64 nm absorption peak characterized as π - π^* transition and 613.57 nm absorption peak from HOMO \rightarrow LUMO (93%) (Table 2a).

Table 1. Selected geometries of the studied molecules at B3LYP/6-31G** level: Bond length (Å), bond angle and dihedral angle (°)

Bond length	A = Thiophene			A = 2-Benzothiophene			A = Benzene		
	C=S	C=O	CH ₂	C=S	C=O	CH ₂	C=S	C=O	CH ₂
C ₁ -S ₁ (C ₆ -S ₂)	1.774	1.777	1.772	1.774	1.778	1.776	1.775	1.777	1.770
C ₄ -S ₁ (C ₅ -S ₂)	1.714	1.715	1.725	1.715	1.714	1.727	1.714	1.715	1.727
C ₁ -C ₂ (C ₆ -C ₇)	1.377	1.381	1.383	1.383	1.385	1.383	1.378	1.382	1.380
C ₂ -C ₃ (C ₇ -C ₈)	1.412	1.410	1.409	1.414	1.410	1.409	1.412	1.407	1.411
C ₃ -C ₄ (C ₅ -C ₈)	1.388	1.382	1.385	1.391	1.389	1.385	1.388	1.381	1.384
C ₄ -C ₅	1.452	1.454	1.435	1.451	1.455	1.438	1.452	1.454	1.440
C ₃ -X (C ₈ -X)	1.479	1.506	1.516	1.479	1.508	1.515	1.478	1.507	1.515
C ₁ -A (C ₆ -A)	1.459	1.458	1.445	1.464	1.463	1.446	1.465	1.464	1.465
C ₁ S ₁ C ₄ (C ₅ S ₂ C ₆)	91.21	91.34	90.80	91.40	91.34	90.86	91.28	91.42	90.97
C ₁ C ₂ C ₃ (C ₆ C ₇ C ₈)	112.63	113.65	113.07	112.71	113.98	113.15	112.76	112.95	113.13
C ₂ C ₃ C ₄ (C ₇ C ₈ C ₅)	113.37	113.78	113.00	113.45	113.64	113.06	113.34	113.62	113.13
C ₃ C ₄ C ₅ (C ₇ C ₅ C ₄)	108.64	109.56	109.35	108.63	109.34	109.26	108.62	109.40	109.24
C ₃ XC ₈	104.61	103.73	101.80	104.59	103.76	101.80	104.57	103.86	101.78
C ₁ S ₁ C ₄ C ₅ (C ₆ S ₂ C ₅ C ₄)	0.56	0.00	0.00	0.76	0.00	0.93	0.51	0.00	0.41
C ₁ C ₂ C ₃ X (C ₆ C ₇ C ₈ X)	178.26	179.96	180.00	179.99	180.00	177.01	178.94	180.00	179.20
C ₂ C ₃ C ₄ C ₅ (C ₇ C ₈ C ₅ C ₄)	178.63	179.84	180.00	179.89	180.00	177.16	179.47	180.00	179.76
C ₁ C ₂ C ₃ C ₄ (C ₆ C ₇ C ₈ C ₅)	0.30	0.03	0.00	-0.05	0.00	0.10	0.02	0.00	-0.06
C ₄ C ₃ XC ₈ (C ₃ C ₈ XC ₃)	-0.18	0.21	0.00	0.22	0.00	0.34	-0.38	0.00	-0.45
S ₁ C ₄ C ₃ X (S ₂ C ₅ C ₈ X)	-179.14	-179.9	180.00	179.45	180.00	-178.54	-179.63	180.00	-179.75
S ₁ C ₁ C ₂ C ₃ (S ₂ C ₆ C ₇ C ₈)	0.12	-0.10	0.00	0.57	0.00	0.59	-0.35	0.00	0.36

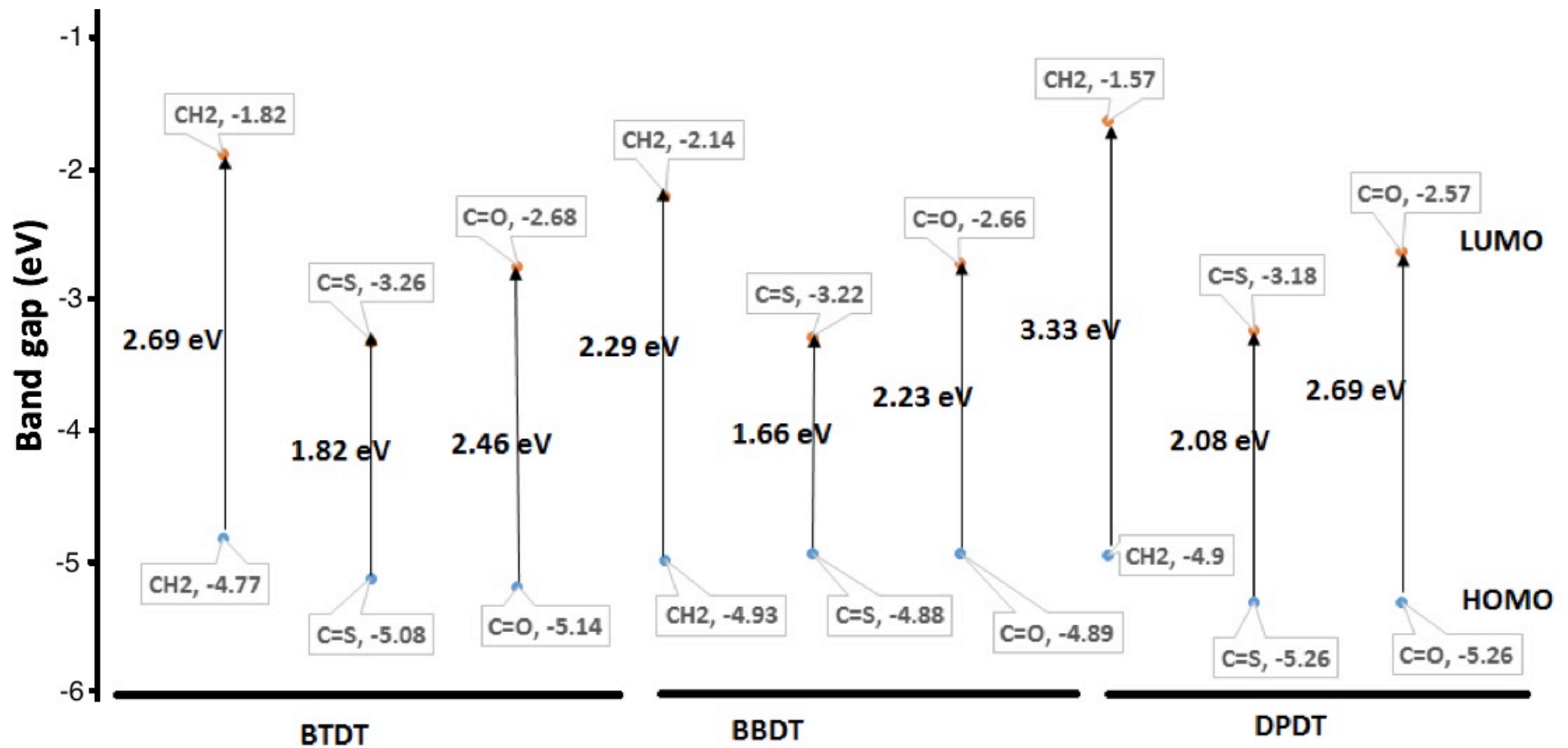


Figure 2. Frontier molecular orbital energy diagram

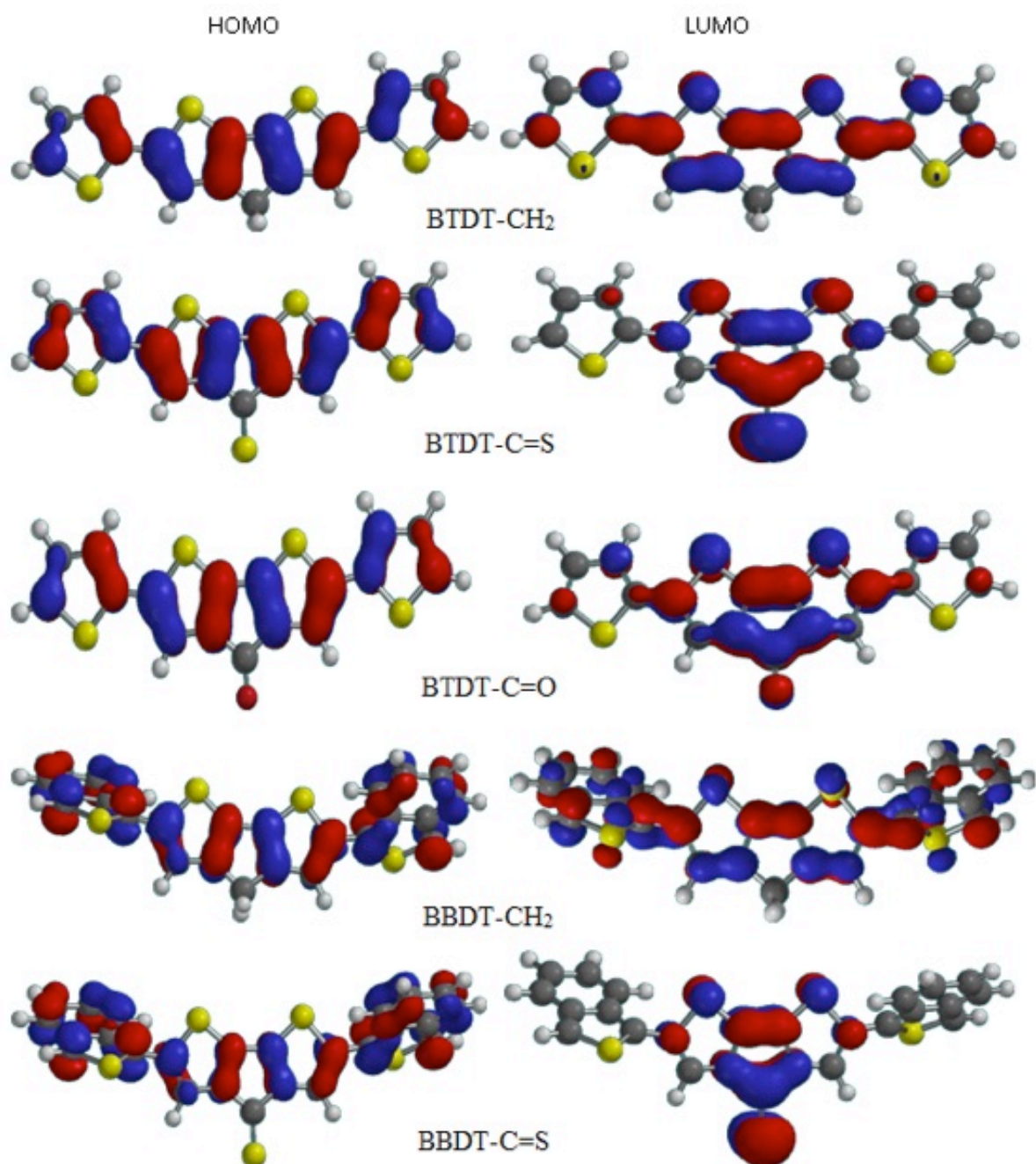


Figure 3. The contour plots of HOMO and LUMO orbitals BTDT, BBDT and DPDT series

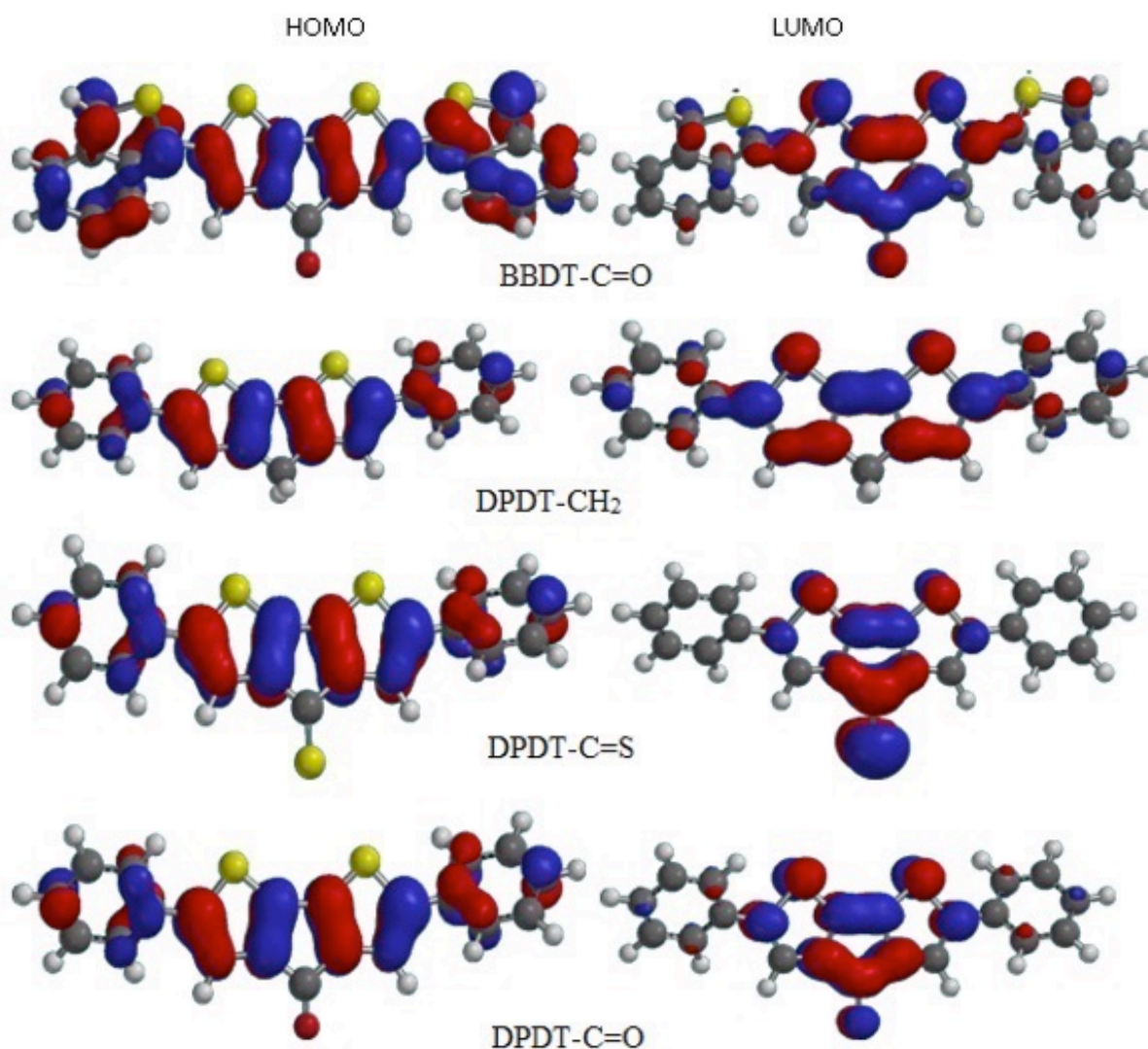


Figure 3. The contour plots of HOMO and LUMO orbitals BTDT, BBDT and DPDT series (continued)

Table 2a. Calculated absorption peaks, oscillation strength and Molecular orbitals (MOs) involved in transition calculated for BTDT at TD-B3LYP/6-31G**

λ_{\max} (mn)	OS	MOs involved in transition
		CH₂
270.85	0.0058	HOMO-2 → LUMO (91%)
289.75	0.0022	HOMO-1 → LUMO (57%)
		HOMO → LUMO+1 (30%)
290.77	0.0012	HOMO → LUMO+2 (73%)
352.92	0.0012	HOMO → LUMO+1 (61%)
		HOMO-1 → LUMO (37%)
413.51	1.8681	HOMO → LUMO (97%)
		C=S
369.43	0.0011	HOMO-5 → LUMO (53%)
		HOMO-3 → LUMO (46%)

370.21	0.7145	HOMO-4 → LUMO (73%) HOMO → LUMO+1 (21%)
392.42	0.6385	HOMO → LUMO+1 (64%) HOMO-4 → LUMO (20%) HOMO-6 → LUMO (11%)
1013.66	0.0478	HOMO → LUMO (97%)
C=O		
316.82	0.0020	HOMO → LUMO+2 (59%) HOMO-3 → LUMO (23%)
317.60	0.1944	HOMO-2 → LUMO (70%) HOMO-4 → LUMO (16%)
363.64	1.1390	HOMO → LUMO+1 (89%)
613.57	0.2513	HOMO → LUMO (93%)

Table 2b. Calculated absorption peaks, oscillation strength and Molecular orbitals (MOs) involved in transition calculated for BBDT at TD-B3LYP/6-31G**

λ_{\max} (nm)	OS	MOs involved in transition
CH₂		
309.87	0.0301	HOMO-2 → LUMO (48%) HOMO → LUMO+4 (21%) HOMO → LUMO+2 (11%) HOMO-1 → LUMO+1 (10%)
349.02	0.1348	HOMO-1 → LUMO+1 (79%) HOMO-2 → LUMO (19%)
369.65	0.0241	HOMO-1 → LUMO (70%) HOMO → LUMO+1 (22%)
374.20	0.1874	HOMO → LUMO+2 (79%)
452.48	0.0120	HOMO → LUMO+1 (73%) HOMO-1 → LUMO (25%)
491.72	1.4963	HOMO → LUMO (97%)
C=S		
429.75	0.0061	HOMO → LUMO+2 (79%) HOMO-1 → LUMO+1 (17%)
464.23	1.1332	HOMO → LUMO+1 (95%)
484.48	0.0162	HOMO-3 → LUMO (97%)
1097.66	0.0643	HOMO → LUMO (97%)
C=O		
389.60	0.0076	HOMO-2 → LUMO (88%)
413.60	0.0076	HOMO → LUMO+2 (74%)
451.32	0.8512	HOMO → LUMO+1 (91%)
503.21	0.0011	HOMO-1 → LUMO (84%)
671.35	0.3459	HOMO → LUMO (92%)

All transitions are from low absorption band in BBDT series. For BBDT-CH₂, the 349.02 nm absorption peak (with 0.1348 O.S value) arises from HOMO+1 → LUMO+1(79%) and HOMO-2 → LUMO (19%); 374.20 nm absorption peak (with 0.1874 O.S value) arises from

HOMO → LUMO+2 (79%) and 491.72 nm with highest O.S value is characterized as π - π^* transition arise from HOMO → LUMO (97%). For BBDT-C=S, the 464.23 nm absorption peak (with highest O.S value) is characterized as π - π^* transition arising from HOMO → LUMO+1 (95%); 484.48 nm absorption peak is from HOMO-3 → LUMO (97%) and 1097.66 nm (the longest absorption peak) is from HOMO → LUMO (97%). For BBDT-C=O, 389.60, 413.60, 451.32 and 671.35 nm absorption peaks are from HOMO-2 → LUMO (88%), HOMO → LUMO+2 (74%), HOMO → LUMO (91%) and HOMO → LUMO (92%) respectively. The 451.32 nm absorption peak with highest O.S value is characterized as π - π^* transition (Table 2b).

Table 2c. Calculated absorption peaks, oscillation strength and Molecular orbitals (MOs) involved in transition calculated for DPDT at TD-B3LYP/6-31G**

λ_{\max} (nm)	OS	MOs involved in transition
CH₂		
281.11	0.0020	HOMO → LUMO+4 (68%)
290.93	0.0061	HOMO → LUMO+3 (87%)
297.84	0.0132	HOMO → LUMO+2 (83%)
314.21	0.0033	HOMO → LUMO+1 (72%) HOMO-1 → LUMO (24%)
377.98	1.7160	HOMO → LUMO (97%)
C=S		
342.69	1.2243	HOMO → LUMO+1 (48%) HOMO-6 → LUMO (24%) HOMO-7 → LUMO (58%)
360.43	0.0486	HOMO-4 → LUMO (65%) HOMO-6 → LUMO (32%)
369.85	0.0449	HOMO-4 → LUMO (41%) HOMO-6 → LUMO (35%) HOMO → LUMO+1 (23%)
874.75	0.0371	HOMO → LUMO (97%)
C=O		
300.92	0.5375	HOMO-5 → LUMO (84%)
310.78	0.1001	HOMO-3 → LUMO (82%)
338.67	0.9251	HOMO → LUMO+1 (86%)
568.63	0.2094	HOMO → LUMO (94%)

For DPDT series, DPDT-CH₂ has three strong absorption peaks at 290.93, 297.84 and 377.98 nm. The 290.93 nm absorption peak arises from HOMO → LUMO+3 (87%), 297.84 nm absorption peak from HOMO → LUMO+3 (83%) and 377.98 nm absorption peak (with highest O.S value) arises from HOMO → LUMO (97%) is characterized as π - π^* transition. For DPDT-C=S, all transitions arising from low absorption bands; the 342.69 nm absorption peak is from HOMO → LUMO+1 (48%), HOMO-6 → LUMO (24%) and HOMO-7 → LUMO (58%); 360.43 nm absorption peak arises from HOMO-4 → LUMO (65%) and HOMO-6 → LUMO (32%); 369.85 nm peak is from HOMO-4 → LUMO (41%), HOMO-6 → LUMO (35%) and HOMO → LUMO+1 (23%) and the longest absorption wave-length (874.75 nm) arises from HOMO → LUMO (97%). DPDT-C=O also shows strong absorptions for all

transitions (i.e. > 0.005 O.S), the 300.92, 310.78, 338.67 and 568.63 nm absorption peaks are from HOMO-5 → LUMO (84%), HOMO-3 → LUMO (82%), HOMO → LUMO+1 (86%) and HOMO → LUMO (94%) respectively. Therefore, the absorption peak with highest O.S value arising from HOMO → LUMO+1 is characterized as π- and n-π* transitions (Table 2c). All molecules are shifted to longer wavelength compared to molecules with CH₂ bridge and molecules with C=S bridge have the longest λ_{max}.

Polarizability and Nonlinear properties

The Polarizability (α), hyperpolarizability (β) and the electric dipole moment (μ) of BTDT, BBDT and DPDT series are calculated at B3LYP/6-31G** to determine non-linear optical (NLO) properties of the studied molecules, the strength of molecular interactions as well as the cross-sections of different scattering and collision processes [38, 39] in an applied electric field based on the finite-field approach [40]. The total static dipole moment μ, the mean polarizability (α₀), the anisotropy of the polarizability (Δα) and the mean first hyperpolarizability (β₀) using the x, y, z components they are defined as equation below.

$$\mu = (\mu_x^2 + \mu_y^2 + \mu_z^2)^{\frac{1}{2}}$$

$$\alpha_0 = \frac{\alpha_{xx} + \alpha_{yy} + \alpha_{zz}}{3}$$

$$\Delta\alpha = \frac{1}{\sqrt{2}} \left[(\alpha_{xx} - \alpha_{yy})^2 + (\alpha_{yy} - \alpha_{zz})^2 + (\alpha_{zz} - \alpha_{xx})^2 + 6\alpha_{xz}^2 + 6\alpha_{xy}^2 + 6\alpha_{yz}^2 \right]^{\frac{1}{2}}$$

$$\beta_0 = (\beta_x^2 + \beta_y^2 + \beta_z^2)^{\frac{1}{2}}$$

$$\beta_x = \beta_{xxx} + \beta_{xyy} + \beta_{xzz}$$

$$\beta_y = \beta_{yyy} + \beta_{xxy} + \beta_{yzz}$$

$$\beta_z = \beta_{zzz} + \beta_{xxz} + \beta_{yyz}$$

$$\beta_0 = (\beta_x^2 + \beta_y^2 + \beta_z^2)^{\frac{1}{2}}$$

The dipole moment μ, mean polarizability (α₀), anisotropy of the polarizability (Δα) and the mean first hyperpolarizability (β₀) for bis(2-benzothiophen-1-yl)-4H-cyclopenta[2,1-b,3;4-b]dithiophene (BBDT), diphenyl-4H-cyclopenta[2,1-b,3;4-b]dithiophene (DPDT) and bis(2-thienyl)-4H-cyclopenta[2,1-b,3;4-b]dithiophene (BTDT) derivatives are listed in Table 3. The magnitude and direction of dipole moment (μ) of a monomer or light weight organic molecules have been considered as one of the parameters for their selection for electro-polymerization, electrochemical properties and solvent interactions [41,42]. Thus, the calculated values of the electric dipole moment of the studied molecules listed in Table 3 revealed that C=O and C=S bridges are electron withdrawing in nature. The comparative size of the dipole moment vectors for the molecules is as follows: -CH₂ < C=S < C=O in each series.

The calculated mean polarizability (α₀) values are 4.15x10⁻²³, 4.47 x10⁻²³ and 4.13 x10⁻²³ esu for BTDT-CH₂, BTDT-C=S and BTDT-C=O; 5.78x10⁻²³, 6.23 x10⁻²³ and 5.99 x10⁻²³ esu

for BBDT-CH₂, BBDT-C=S and BBDT-C=O; 3.78x10⁻²³, 4.43x10⁻²³ and 4.22x10⁻²³ esu for BPDT-CH₂, BPDT-C=S and BPDT-C=O respectively. The polarizability (α_0) values for the molecules are as follows: -CH₂ < C=O < C=S bridge in each series, indicating that polarizability (α_0) is directly proportional to absorption wavelength and inversely proportional to the energy band gap. Thus the higher the polarizability value the longer the λ_{max} nm and the lower the energy band gap (Tables 2 and 3). The first hyperpolarizability (β_0) values are 4.84x10⁻³⁰, 3.91x10⁻³⁰ and 6.56x10⁻³⁰ esu for BTDT-CH₂, BTDT-C=S and BTDT-C=O; 4.52x10⁻³⁰, 4.60x10⁻³⁰ and 6.67x10⁻³⁰ esu for BBDT-CH₂, BBDT-C=S and BBDT-C=O; 1.53x10⁻³⁰, 4.00x10⁻³³ and 5.46x10⁻³⁰ esu for BPDT-CH₂, BPDT-C=S and BPDT-C=O respectively. The magnitude of the molecular hyperpolarizability β_0 , which is one of dominant key factors in a nonlinear optical (NLO) system shows that molecular structures with X = (C=O) could be best NLO material in each series.

CONFLICT OF INTEREST

Authors declare no competing interests.

CONCLUSION

In this work, three series of symmetrical molecules containing 4H-cyclopenta[2,1-b,3;4-b]dithiophene as π -center are studied at B3LYP/6-31G** level of calculations. The results showed that the geometries of the π -center of the studied molecules are affected by both A and X, although the effect of X is more pronounced. The HOMO and LUMO are destabilized in C=O and C=S bridges which result in blue shifting in the absorption spectrum. In each series, molecules with C=S bridge presented lowest band gaps and longest wave lengths, therefore BBDT-C=S and BTDT-C=S could be employed in solar cells (i.e. band gap < 1.9 eV) and optical devices. However, the values of molecular hyperpolarizability (β_0) calculated show that molecules with C=O bridge could be best suitable as NLO material.

Table 3. The electric dipole moment μ (au), the average polarizability α_0 (1a.u = 0.1482×10^{-24} esu) and the first hyperpolarizability β_0 (1a.u = 8.6393×10^{-33} esu esu) for α, α -bis(2-benzothiophen-1-yl)-4H-cyclopenta[2,1-b,3,4-b']dithiophene derivatives

A X Parameters	Thiophene			Benzothiophene			Benzene		
	CH ₂	C=S	C=O	CH ₂	C=S	C=O	CH ₂	C=S	C=O
μ_x	2.10×10^{-5}	-6.15×10^{-3}	-2.67×10^{-4}	2.60×10^{-4}	-7.00×10^{-6}	-2.50×10^{-5}	2.87×10^{-3}	-2.17×10^{-3}	2.00×10^{-6}
μ_y	-0.17	1.04	1.59	0.22	0.86	1.27	0.45	0.09	-1.36
μ_z	-3.00×10^{-6}	-6.15×10^{-3}	-7.13×10^{-5}	-0.30	-0.43	-0.80	0.13	-0.14	1.00×10^{-6}
μ (Debye)	0.44	2.64	4.04	0.95	2.43	3.82	1.18	2.19	3.45
α_{xx}	570.58	523.15	535.449	706.64	683.12	705.05	481.72	513.85	562.02
α_{xy}	-5.50×10^{-3}	-1.39	-0.09	0.35	-0.02	-0.02	-0.42	0.20	-0.02
α_{yy}	233.72	302.41	229.14	356.84	408.41	367.27	202.53	314.22	257.82
α_{xz}	0.01	0.71	0.65	-0.41	0.02	0.010	-0.07	-0.08	0.02
α_{yz}	-1.43×10^{-4}	1.80	0.09	1.60	3.26	12.13	-13.45	-15.36	-2.18×10^{-4}
α_{zz}	36.51	79.50	72.36	106.90	169.92	124.94	80.32	67.70	35.14
$\Delta\alpha$	467.76	384.21	407.96	521.79	444.84	505.09	357.13	388.00	458.11
α_0 (esu)	4.15×10^{-23}	4.47×10^{-23}	4.13×10^{-23}	5.78×10^{-23}	6.23×10^{-23}	5.99×10^{-23}	3.78×10^{-23}	4.43×10^{-23}	4.22×10^{-23}
β_{xxx}	-3.43	56.19	3.62	-40.80	7.19	11.21	34.49	-12.83	1.57
β_{xyy}	2.33	-9.49	7.06	14.16	7.50	7.72	2.58	6.81	4.56
β_{xzz}	-4.92	-9.29	0.97	-1.98	-7.04	-4.24	-3.89	-4.54	-7.83
β_{yyy}	-30.33	75.82	-2.56	123.73	-42.12	-105.20	-67.71	-112.79	-37.17
β_{yxx}	-534.08	-406.84	-738.61	-211.91	250.53	39.44	254.20	145.58	685.17
β_{yzz}	4.43	-35.80	-18.28	17.88	-22.32	-24.86	-21.22	4.06	-15.98
β_{zxx}	-0.01	-15.66	-1.73	-628.83	655.49	877.58	92.51	64.61	-0.01
β_{zyy}	-0.00	2.81	0.05	41.31	-86.80	-42.51	-13.18	-17.93	0.00
β_{zzz}	0.52	-6.71	0.00	66.67	-69.62	-68.90	-23.70	-2.56	0.14
β_x	-6.03	37.40	11.66	-28.61	7.641	14.68	33.18	-10.57	-1.70
β_y	-559.98	-366.82	-759.45	-70.31	186.09	-90.63	165.27	36.85	632.02
β_z	0.51	-19.57	-1.68	-520.85	499.07	766.17	55.63	44.12	0.14
β_0 (au)	560.01	369.24	759.54	526.35	532.61	771.65	177.51	58.44	632.02
β_0 (esu)	4.84×10^{-30}	3.19×10^{-30}	6.56×10^{-30}	4.52×10^{-30}	4.60×10^{-30}	6.67×10^{-30}	1.53×10^{-30}	4.00×10^{-33}	5.46×10^{-30}

REFERENCES

- [1] G. Tourillon, Polythiophene and its derivatives, in: T.A. Skotheim (Ed.), Handbook of Conducting Polymers, vol. 1 (Dekke, Inc., New York, 1986)
- [2] P. Baeuerle, Oligothiophenes in electronic materials, in: G. Wegner, K. Muellen (Eds.), The Oligomeric Approach, (Wiley-VCH, Weinheim, 1998).
- [3] P. de Silva, H.Q.N. Gunaratne, T. Gunnlaugsson, A.J.M. Huxely, C.P. McCoy, J.T. Rademacher, T.E. Rice, *Chem. Rev.*, **1997**, 97, 1515.
- [4] C.E. Kerr, C.D. Mitchell, J. Headrick, B.E. Eaton, T.L. Netzel, *J. Phys. Chem. B.*, **2000**, 104, 1637.
- [5] U. Stalmach, H. Detert, H. Meier, V. Gebhardt, D. Haarer, A. Bacher, H.-W. Schmidt, *Opt. Mater.* **1998**, 9, 77.
- [6] M. Leuze, M. Hohloch, M. Hanack, *Chem. Mater.* **2002**, 14, 3339).
- [7] R.H. Young, C.W. Tang, A.P. Marchetti, *Appl. Phys. Lett.*, **2002**, 80, 874.
- [8] W. Li, Z. Wang, P. Lu, *Opt. Mater.*, **2004**, 26, 243.
- [9] F. Garnier, G. Horowitz, D. Fichou, A. Yassar, *Synth. Met.*, **1996**, 81, 163.
- [10] X.-C. Li, H. Cherringhaus, F. Garnier, et al., *J. Am. Chem. Soc.*, **1998**, 120, 2206.
- [11] I.S. Moreira, D.W. Franco, *J. Chem. Soc. Chem. Commun.*, **1992**, 5, 450-451.
- [12] K. Takahashi, T. Nihira, K. Akiyama, Y. Ikegami, E. Fukuyo, *J. Chem. Soc. Chem. Commun.*, **1992**, 8, 620-622.
- [13] (a) O.-K. Kim, K.-S. Lee, Z. Huang, W.B. Heuer, C.S. Paik-Sung, *Opt. Mater.*, **2002**, 21(1-3), 559-564; (b) O-K Kim, H. Y. Woo, J.-K. Kim, W. B. Heuer, K.-S. Lee, C.-Y. Kim, *Chem. Phys. Lett.*, **2002**, 364(5-6), 432-437.
- [14] P. Lu and G.M. Xia *J. Serb. Chem. Soc.* **2005**, 70(2), 201-208.
- [15] M. Guang, G.M. Xia, Q. Fang, X.G. Xui, G.B. Xui, W. Wangi, Z.Q. Liu, G.L. Song and Y.J. Wu, *Chinese Chem. Lett.*, **2003**, 14(6), 657.
- [16] G.-M. Xia, P. Lu and S.-Q. Liu, *Acta Chim. Slov.*, **2005**, 52, 336.
- [17] R.P. Ortiz, M.C.R. Delgado, J. Casado, V. Hernandez, O.-K. Kim, H.Y. Woo and J.T.L. Navarrete, *J. Am. Chem. Soc.*, **2004**, 126, 13363.
- [18] J. Casado, H.E. Katz, V. Hernández, J.T. López Navarrete, *J Phys. Chem B.*, **2002**, 106, 2488.
- [19] A.L. Nei Marc, L. Bernardo, P. Ricardo, D. S. Barbosa, *Int. J. Quant. Chem.*, **2006**, 106, 2723.
- [20] Z. El Malkia, M. Bouachrineb, M. Hamidib, L. Bejjita, and M. Haddad, *J. Sci. Res.*, **2012**, 4(1), 119.
- [21] M. Bouachrine, M. Hamidi, S. M. Bouzzine and H. Taoufik, *J. Appl Chem. Res.* **2009**, 10, 29.
- [22] G. A. Jarlesson, R. G. Jeconias, C. S. C. Sheila, L. Bernardo, D. N. Jordan, *J. Mol. Struct THEOCHEM*, **2006**, 759, 87.
- [23] S.M. Bouzzine, S. Bouzakraoui, M. Bouachrine and M. Hamidi, *J. Mol. Struct. (THEOCHEM)*, **2005**, 726, 271.
- [24] S.M. Bouzzine, M. Hamidi, M. Bouachrine, *Orbital*, **2009**, 1(2), 203-214.
- [25] H.A. Aouchiche, S. Djennane, A. Boucekkine, *Synth. Met.*, **2004**, 140, 127.
- [26] B. Semire, O. A. Odunola and I. A. Adejoro *J. Mol. Modeling*, **2012**, 18(6), 2755.
- [27] B. Semire and O. A. Odunola, *Quimica Nova*, **2014**, 37(5), 833.
- [28] B. Semire and O. A. Odunola. *Indones. J. Chem.*, **2015**, 15 (1), 93 – 100.
- [29] A.D. Becke, *J. Chem. Phys.* **1993**, 98, 5648.
- [30] C. Lee, W. Yang, R.G. Parr, *Phys. Rev. B.*, **1988**, 37, 785.

- [31] Spartan 14, *Wavefunction*, INC, Irvine CA 92612, USA
- [32] D. Mühlbacher, M. Scharber, M. Morana, Z. Zhu, D. Waller, D.R. Gaudiana, C. Brabec, *Adv. Mater.*, **2006**, 18, 2884.
- [33] T.T. Steckler, K.A. Abboud, M. Craps, A.G. Rinzler, *J. Reynolds, Chem. Commun.* **2007**, 46, 4904.
- [34] P.F. Xia, X.J. Feng, J. Lu, S.W. Tsang, R. Movileanu, Y. Tao, M.S. Wong, *Adv. Mater.*, **2008**, 20, 4810.
- [35] .B. Asbury, Y.Q. Wang Y,E. Hao, H. Ghosh, T. Lian, *Res Chem Intermed*, **2001**, 27, 393-406.
- [36] Z. Wu, B.Fan, F. Xue, C.Adachi, J. Ouyang, *Energy Mater. Sol. Cells*, **2010**, 94, 2230.
- [37] A.Gadisa, M.Svensson, M.R.Andersson, O.Inganas, *Appl. Phys. Lett.*, **2004**, 4, 1609.
- [38] Y. Sun, X. Chen, L. Sun, X. Guo, W. Lu, *Chem. Phys. Lett.*, **2003**, 38, 397.
- [39] C.R. Zhang, H.S. Chen, G.H. Wang, *Chem. Res. Chin. U.*, **2004**, 20, 640.
- [40] Y.X. Sun, Q.L. Hao, W.X. Wei, Z.X. Yu, L.D. Lu, X. Wang, Y.S. Wang, *J. Mol. Struct.: (THEOCHEM).*, **2009**, 904, 74.
- [41] H. Nikoofard and H. Sabzyan, *J. Fluorine Chem.*, **2007**, 128(6), 668-673.
- [42] W.H. Meyer, H. Kiess, B. Binggeli, E. Meier and G. Harbeke, *Synth. Met.*, **1985**, 10(4), 255.